ACCOUNTS of chemical research

Article

Cite This: Acc. Chem. Res. 2018, 51, 1571−1580

pubs.acs.org/accounts

Innovative Strategies for Electrocatalytic Water Splitting

Bo You* and Yujie Sun*

Department of Chemistry and Biochemistry, Utah State University, Logan, Utah 84322, United States

CONSPECTUS: Electrocatalytic water splitting driven by renewable energy input to produce clean H_2 has been widely viewed as a promising strategy of the future energy portfolio. Currently, the state-of-the-art electrocatalysts for water splitting in acidic solutions are IrO_2 or RuO_2 for the O_2 evolution reaction (OER) and Pt for the H_2 evolution reaction (HER). Realization of large-scale H_2 production from water splitting requires competent nonprecious electrocatalysts. Despite the advances of decades in this field, several challenges still exist and need to be overcome: (1) Most efforts in the design of nonprecious electrocatalysts have focused on developing HER catalysts for acidic conditions but OER catalysts for alkaline conditions owing to their thermodynamic convenience, potentially resulting in incompatible integration of the two types of catalysts and thus inferior overall performance. (2) In conventional water electrolysis, HER and OER are strictly coupled and therefore H_2 and O_2 are produced simultaneously, which may lead to explosive H_2/O_2 mixing due to gas crossover. Meanwhile, the coexistence of H_2, O_2, and electrocatalysts could produce reactive oxygen species that might shorten the lifetime of an electrolyzer. (3) The HER rate is often limited by that of OER due to the more sluggish kinetics of the latter, which lowers the overall energy conversion efficiency. Moreover, the product of OER, O_2, is not highly valuable. (4) It remains challenging to develop efficient and low-cost H_2 storage and transport systems for the future H_2 economy.

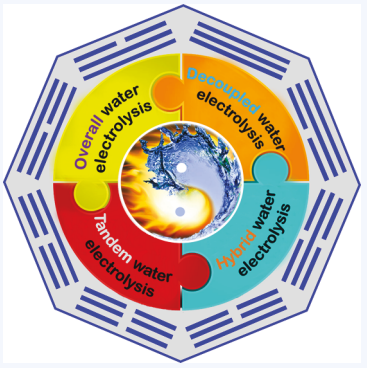

In this Account, we describe recent progress in innovative strategies to address the aforementioned four challenges in conventional water electrolysis. These novel strategies include (1) *overall water electrolysis* based on bifunctional nonprecious electrocatalysts (or precursors) to drive both HER and OER under the same conditions, (2) *decoupled water electrolysis* achieved by redox mediators for temporally and spatially separating HER from OER, (3) *hybrid water electrolysis* by integrating thermodynamically more favorable organic upgrading reactions to replace OER, and (4) *tandem water electrolysis* by utilizing biocatalysts for converting the in situ produced H_2 with foreign compounds (e.g., CO_2 and N_2) to more valuable products. Finally, the remaining challenges and future perspectives are also presented. We hope this Account will function as a momentum call for more endeavors into the development of advanced electrocatalytic systems and novel strategies for practicable H_2 production from water as well as the electrocatalytic upgrading of diverse organic compounds.

1. INTRODUCTION

Along with the rise of population and the development of economy, global energy demand will increase continuously in the foreseeable future.[1,2] The vast majority of contemporary energy sources are derived from fossil fuels such as coal, oil, and natural gas. However, the depletion of nonrenewable fossil fuels and the detrimental effects of fossil fuel utilization on the environment have stimulated intense research in innovative technologies for the conversion and storage of sustainable and clean energy sources, like solar and wind.[1−3] To address the intermittency issue of renewable energy, electrocatalytic generation of H_2 from water has been considered as an attractive approach.[4−6] In order to alleviate charge transport losses during electrochemical processes, traditional water electrolysis is usually carried out under either acidic conditions with a proton exchange membrane (PEM) or in alkaline media with a diaphragm (Figure 1a).[4,5] Depending on the reaction conditions, the two half-reactions for water splitting can be expressed in different ways (Figure 1b). Under standard conditions, a thermodynamic potential of 1.23 V is required to drive electrochemical water splitting (Figure 1b), which corresponds to an energy input of ΔG = 237.1 kJ mol^{-1}.

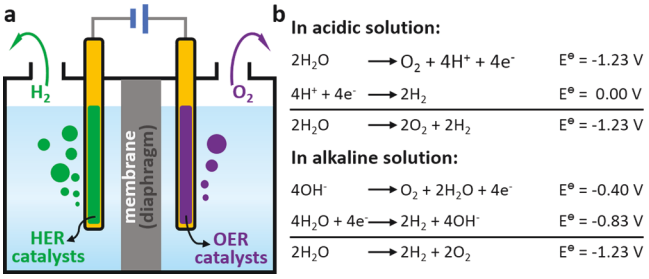

Figure 1. (a) Scheme of conventional water electrolyzers. (b) Water splitting reactions under acidic and alkaline conditions.

Unfortunately, the sluggish kinetics of both H_2 evolution reaction (HER) and O_2 evolution reaction (OER) require high overpotentials to reach appreciable current density, resulting in relatively low energy conversion efficiencies. Thus, the input potential of water splitting in practical electrolyzers is much larger than 1.23 V. In addition, electrocatalysts are usually

Received: January 1, 2018
Published: March 14, 2018

DOI: 10.1021/acs.accounts.8b00002
Acc. Chem. Res. 2018, 51, 1571−1580

needed such as noble metal-based catalysts (e.g., Pt for HER and IrO_2 or RuO_2 for OER) for acidic media and transition metal-based catalysts (e.g., Ni electrodes for HER and stainless steel composites for OER) for alkaline electrolytes (Figure 1).[7] However, the prohibitive cost, scarce reserve, and unsatisfactory stability of noble metal-based electrocatalysts, as well as the mediocre activity of noble metal-free electrocatalysts, hinder large-scale H_2 production through water electrolysis.[4−6]

Indeed, enormous efforts have been made to develop nonprecious electrocatalysts with improved HER and OER performance.[4−6] For example, metal alloys, borides, carbides, nitrides, phosphides, and chalcogenides have been explored as competitive HER electrocatalysts in acidic solutions,[5,6] while many nonprecious OER catalysts of metal oxides and (oxy)hydroxides have been reported with promising activities in alkaline media.[2] Nevertheless, numerous challenges still exist: (1) The prevalent strategies for nonprecious catalyst development often lead to incompatible or complicated integration of HER and OER electrocatalysts as they are usually developed under different conditions.[8−13] (2) HER and OER in conventional water electrolysis are strictly coupled, which may result in the formation of explosive H_2/O_2 gas mixtures.[14−19] The gas crossover not only poses safety issues, but also reduces the energy efficiency in that O_2 would be reduced back to water on the cathode side.[7] Meanwhile, the coexistence of gas mixtures and electrocatalysts may generate reactive oxygen species, which can degrade the membrane and cause premature device failure.[14] (3) Since OER is a four-electron process, it requires much higher overpotential than HER to afford the same current density. Ironically, the product of OER, O_2, is not highly valuable.[20−25] (4) It is still challenging to obtain cost-effective H_2 storage and transport systems for its use on demand.[26,27]

In this Account, we summarize recent advances in nonconventional water electrolysis to tackle the aforementioned four challenges. Four innovative strategies termed as *overall water electrolysis*, *decoupled water electrolysis*, *hybrid water electrolysis*, and *tandem water electrolysis* will be presented (Figure 2), with an emphasis on rationally designing earth-abundant electrocatalysts, constructing novel electrolyzer modules, and tailoring the reaction interfaces.

2. NONCONVENTIONAL WATER ELECTROLYSIS

2.1. Overall Water Electrolysis

Based on the Nernst equation, acidic conditions are favorable toward HER, while OER proceeds more easily in alkaline media. Therefore, most efforts in developing HER and OER electrocatalysts are conducted in acidic and alkaline electrolytes, respectively. However, in order to accomplish water electrolysis, both HER and OER electrocatalysts are preferred to function in the same electrolyte. The disparity of conditions during the development stage of HER and OER catalysts will likely result in complicated integration and mediocre performance for full water splitting.[28] With these considerations in mind, our group is interested in developing nonprecious bifunctional electrocatalysts for both HER and OER in the same electrolyte to achieve efficient overall water electrolysis (Figure 2a), due to the advantages of simplifying the electrolyzer configuration and reducing the overall cost. Owing to the nature of a four-electron process, the overpotential of OER is typically much higher than that of HER to afford same current density, therefore the overall efficiency of

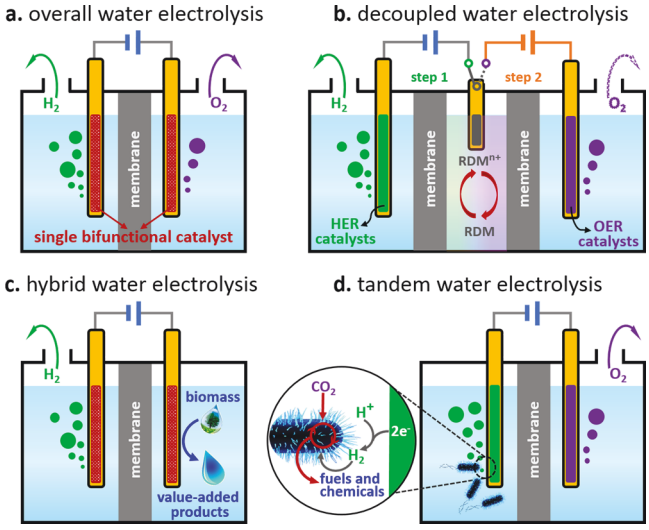

Figure 2. Four innovative strategies for nonconventional water splitting: (a) overall water electrolysis, (b) decoupled water electrolysis, (c) hybrid water electrolysis, and (d) tandem water electrolysis.

water splitting in alkaline media would be better than that in acidic media. Moreover, most earth-abundant OER catalysts cannot survive strong acidic electrolytes.

Following our previous success in preparation of CoS_x[29] and NiS_x films[30] via electrodeposition, a similar potentiodynamic deposition was conducted to obtain Co−P film by consecutive linear scanning between −0.3 and −1.0 V vs Ag/AgCl at a scan rate of 5 mV s^{-1} and a rotation speed of 500 rpm under stirring in the stock solution (50 mM $CoSO_4$, 500 mM NaH_2PO_2, and 100 mM CH_3COONa in water).[8] Scanning electron microscopy (SEM) image and the cross-section SEM image of Co−P reveal nearly complete coverage of Co−P on a copper substrate and thickness of 1−3 μm (Figure 3a). Linear sweep voltammetry (LSV) was conducted to investigate the electrocatalytic HER, OER, and overall water splitting performance of Co−P in 1.0 M KOH. As depicted in Figure 3b, inset, the HER polarization curve of Co−P demonstrates an onset potential of approximately −50 mV vs the reversible hydrogen electrode (RHE), slightly more negative than that of Pt/C (~0 mV vs RHE). However, the catalytic current density of Co−P quickly surpasses that of Pt/C beyond −167 mV vs RHE (Figure 3b), highlighting its remarkable HER activity. Co−P requires an overpotential of only 94 mV to reach 10 mA cm^{-2} and features a small Tafel slope of 42 mV dec^{-1}, representing an impressive performance for HER under alkaline conditions. The SEM image of Co−P after 24 h electrolysis (post-HER Co−P) confirms the retention of its morphology (Figure 3c), implying its robust stability for long-term H_2 evolution. Subsequently, its OER performance was assessed in the same electrolyte (1.0 M KOH). Co−P achieves 10 mA cm^{-2} at an overpotential of 345 mV (Figure 3d), lower than those of IrO_2 and many other nonprecious OER catalysts. In contrast to the uniform morphology of the fresh and post-HER Co−P, the SEM image of the post-OER Co−P indicates particle aggregates (Figure 3e). Further characterizations reveal the oxidation of both Co and P during OER.[8] Therefore, the real active sites for OER are attributed to the in situ generated cobalt oxides and (oxy)hydroxides on the bulk Co−P film. Finally, a water electrolyzer using Co−P as the electrocatalyst (or catalyst precursor) on both anode and cathode was assembled and

DOI: 10.1021/acs.accounts.8b00002
Acc. Chem. Res. 2018, 51, 1571−1580

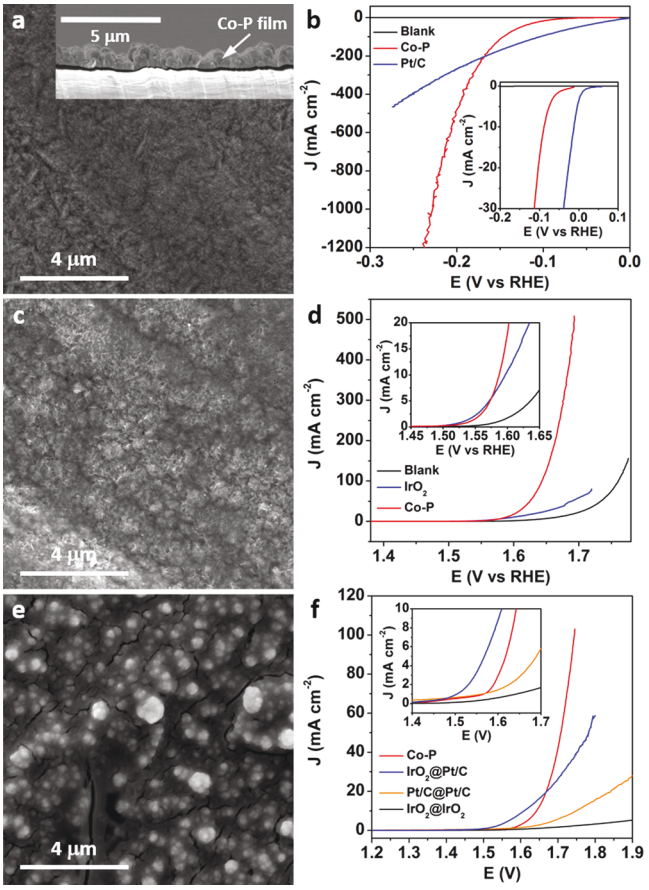

Figure 3. SEM images of (a) fresh Co−P, (c) post-HER Co−P, and (e) post-OER Co−P. LSV curves for (b) HER, (d) OER, and (f) overall water splitting. Reproduced from ref 8. Copyright 2015 John Wiley & Sons, Inc.

tested in 1.0 M KOH. The Co−P catalyst couple demonstrates a cell voltage of only 1.744 V to afford 100 mA cm^{-2}, even lower than that of the Pt/C and IrO_2 couple (Figure 3f). Analogous bifunctional performance for overall water splitting can be obtained from electrodeposited Ni−P film as well.[9]

In order to accelerate electrocatalytic kinetics and lower the required overpotential, an electrocatalyst with optimal reaction interfaces is critical for both triphase HER and OER (solid, liquid, and gas).[10−12] Within this scenario, catalysts featuring large specific surface area, open porous structure, and high accessibility of active sites are anticipated to be beneficial to electrocatalytic performance.[10−12] Therefore, we synthesized three-dimensional (3D) hierarchically porous Ni_2P superstructures on Ni foam (Ni_2P/Ni/NF) as nonprecious bifunctional electrocatalysts for overall water splitting.[10] Ni_2P/Ni/NF was prepared through a template-free electrodeposition of porous metallic Ni microsphere arrays on a Ni foam (Ni/NF) followed by phosphorization (Figure 4a). SEM images corroborate its hierarchical macroporosity and urchin-like morphology (Figure 4b). The cell voltage of a Ni_2P/Ni/NF-based electrolyzer at 10 mA cm^{-2} is 1.49 V (Figure 4f), much lower than those of Co−P (1.64 V)[8] and Ni−P (1.67 V).[9] The exceptional activity of Ni_2P/Ni/NF is ascribed to its unique superstructure. The 3D hierarchically macroporous structure with interconnected configuration not only provides high accessibility of active sites but also buffers electrolyte to facilitate ion transport and gas diffusion.[31,32] In addition, we also explored nickel sulfides as bifunctional electrocatalysts for overall water splitting. High-temperature sulfurization of Ni/NF can readily achieve 3D hierarchically porous NiS_x superstructures (hp-NiS_x, Figure 4c). The hp-NiS_x possesses both macropores and mesopores, in contrast to Ni_2P/Ni/NF with singular macropores. The hp-NiS_x electrocatalyst couple only requires a voltage of 1.47 V to reach 10 mA cm^{-2} for overall water electrolysis (Figure 4f).

Benefiting from high specific surface area, controllable pore texture, and modular organic and inorganic components, metal−organic frameworks (MOFs) represent promising candidates to obtain competent electrocatalysts.[12,33,34] We first reported a MOF-derived route to produce mesoporous Co−P/NC nanopolyhedrons composed of CoP_x nanoparticles embedded in N-doped carbon matrices as bifunctional electrocatalysts for both HER and OER.[12] The Co−P/NC was prepared by direct carbonization of Co-based zeolitic imidazolate frameworks (ZIF-67) followed by phosphorization (Figure 4d). SEM images of Co−P/NC suggest its inheritance of the polyhedron-like morphology of ZIF-67 (Figure 4e). Elemental mapping results (Figure 4e) confirm the presence of Co, P, N, and C in Co−P/NC, and P is highly localized with Co, consistent with the formation of CoP_x. The specific surface area of Co−P/NC is 183 m^2 g^{-1}, larger than that of hp-NiS_x (11 m^2 g^{-1}).[11] As expected, Co−P/NC exhibits remarkable HER and OER activities and affords a current density of 165 mA cm^{-2} at 2.0 V for overall water splitting.[12] Figure 4f compares the cell voltages of overall water electrolysis based on our reported bifunctional electrocatalysts at different current densities, including the Pt/C and RuO_2 couple as a reference. Such a bifunctional electrocatalyst strategy for overall water splitting can be readily extended to other transition metal and noble metal derivatives and even metal-free nanocarbons.[35]

2.2. Decoupled Water Electrolysis

In overall water electrolysis, the production rate of H_2 is still strictly limited by the rate of O_2 evolution, as HER and OER take place simultaneously. However, sometimes it is more desirable to produce H_2 at a much higher rate with a moderate voltage input. Decoupled water electrolysis achieved by redox mediators can temporally and spatially separate HER and OER (Figure 2b), eliminating H_2/O_2 mixing and the formation of reactive oxygen species. Conceptually, when HER takes place on the cathode, the counter reaction is the oxidation of the redox mediator instead of OER. Subsequently, the oxidized redox mediator will be reduced back to its original state at the same electrode, which couples O_2 evolution on another working electrode. Overall, the redox mediator functions as a reversible electron (and proton) donor/acceptor.

Cronin's group reported decoupled water electrolysis in acidic electrolytes using a series of electron-coupled proton buffers such as silicotungstic acid,[14] phosphomolybdic acid,[15] and quinone derivatives.[17] However, acidic medium is highly corrosive and also prohibits the utilization of nonprecious OER catalysts. Our group recently reported that a ferrocene derivative, (ferrocenylmethyl)trimethylammonium chloride (FcNCl, Figure 5b), which is highly soluble in water, can act as a proton-independent electron reservoir to realize decoupled water electrolysis in neutral electrolyte (0.5 M Na_2SO_4). Due to the benign conditions, nonprecious electrocatalysts like Ni_2P, Co−P, and metallic Ni could be adopted to drive both HER and OER. As illustrated in Figure 5a,[16] in step 1, the HER electrode is connected and a negative voltage bias is applied to

DOI: 10.1021/acs.accounts.8b00002
Acc. Chem. Res. 2018, 51, 1571−1580

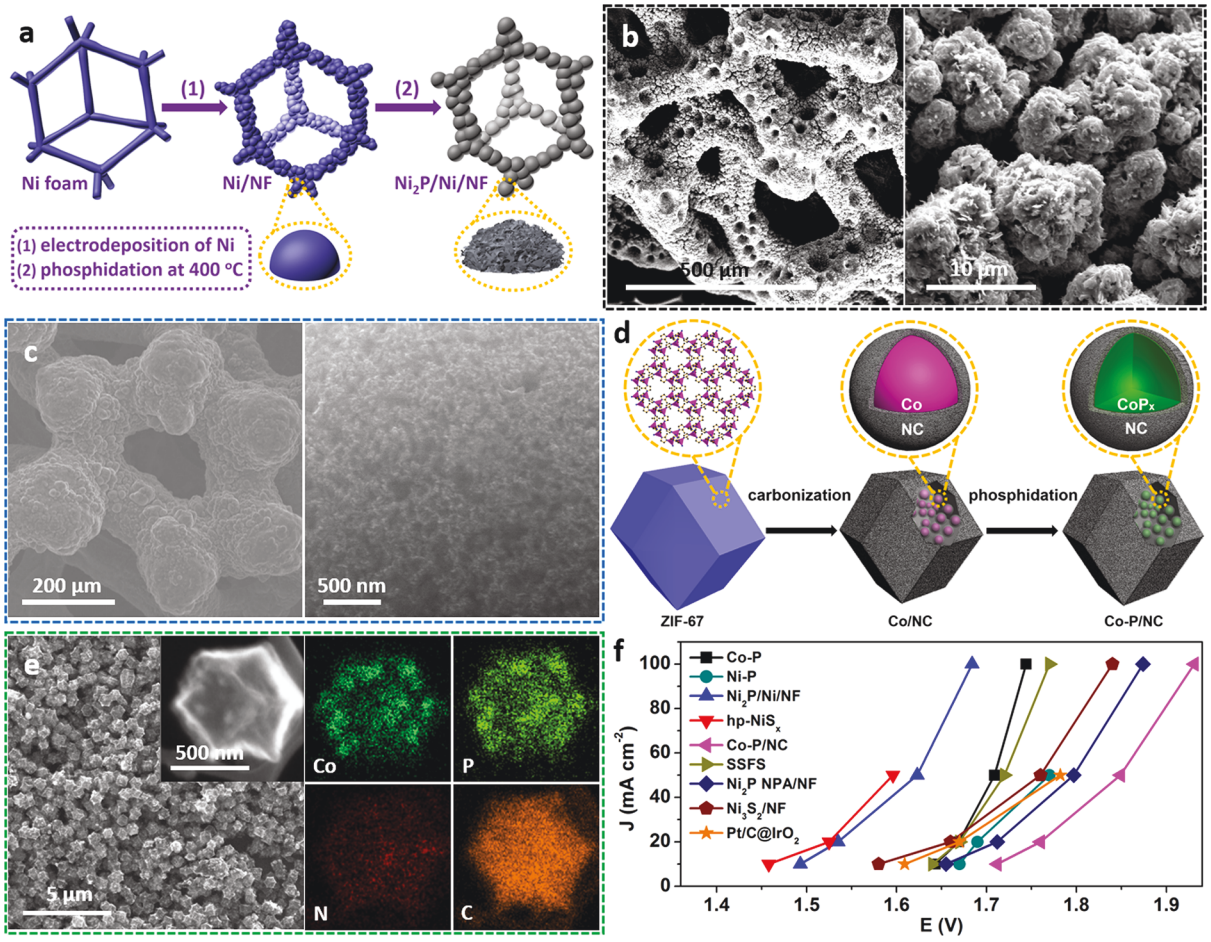

Figure 4. (a) Preparation scheme of Ni_2P/Ni/NF. SEM images of (b) Ni_2P/Ni/NF and (c) hp-NiS_x. (d) Preparation scheme of Co−P/NC. (e) SEM and element mapping images of Co−P/NC. (f) Comparison of cell voltages to achieve benchmark current densities for diverse bifunctional electrocatalysts of overall water splitting.[8−13,21,23] Panel b reproduced from ref 10. Copyright 2016 American Chemical Society. Panel c reproduced from ref 11. Copyright 2016 John Wiley & Sons, Inc. Panels d and e reproduced from ref 12. Copyright 2015 American Chemical Society.

initiate H_2 generation, and simultaneously FcNCl in the counter chamber is oxidized because of its less positive oxidation potential than that of OER (Figure 5c). Figure 5d shows the LSV curves of HER on the Ni_2P/Ni/NF cathode with and without FcNCl in the counter compartment. In the absence of FcNCl, Ni_2P/Ni/NF exhibits an onset voltage of −2.2 V. Upon the addition of 50 mM FcNCl in the counter chamber, the onset voltage shifts to −1.2 V, indicating that the oxidation of FcNCl is significantly easier than OER and nearly 1 V voltage input is saved. Subsequently, in step 2, the OER electrode (a Ni foam) is connected, and a positive voltage bias is applied to drive O_2 evolution on the Ni foam, while the oxidized $FcNCl^+$ is reduced back to FcNCl in the counter chamber. Because the reduction potential of $FcNCl^+$ is more positive than that of HER, the required voltage for OER with FcNCl in the counter chamber is reduced about 1.8 V relative to the case without FcNCl (Figure 5e). Gas chromatography (GC) analysis confirmed 100% Faradaic efficiencies for both steps, and only one gas product was produced each time. The similarity of 20 electrolysis cycles (50 h) indicates the great robustness and negligible crossover of FcNCl as an electron reservoir for long-term decoupled water electrolysis (Figure 5f). When integrated with photovoltaic cells, decoupled water electrolysis can also be driven by sunlight irradiation without external voltage bias (Figure 5g).[16] In addition to FcNCl, we also discovered that $Na_4[Fe(CN)_6]$ can function as an electron reservoir in both neutral and alkaline electrolytes.[16] As alluded in the above discussion, an ideal molecular redox mediator should be low cost and highly soluble in water and features a fast and reversible redox couple that is positioned between the onset potentials of HER and OER. Besides molecular complexes, $Ni(OH)_2$ can also act as a solid-state redox mediator for decoupled water electrolysis, even though the operation is rather complicated and its redox capacity is largely determined by the electrode area and mass loading.[18,19]

2.3. Hybrid Water Electrolysis

Following the aforementioned strategy of decoupled water electrolysis, OER still takes place as the oxidation reaction to complete the electrocatalysis cycle, which requires large overpotential, and its product O_2 does not bear a high price tag. The primary purpose of water oxidation is to extract electrons and transport them to the cathode side for the production of H_2, which is the real desirable product of water splitting. O_2 is merely a side product of the whole process, even though it is responsible for the major energy loss of water electrolysis. In response, we proposed a concept of hybrid water electrolysis by replacing OER with thermodynamically more favorable organic oxidation reactions, wherein biomass-derived intermediates can serve as attractive organic substrates (Figure 2c).[21−24] Such a hybrid water electrolysis strategy possesses at

DOI: 10.1021/acs.accounts.8b00002
Acc. Chem. Res. 2018, 51, 1571−1580

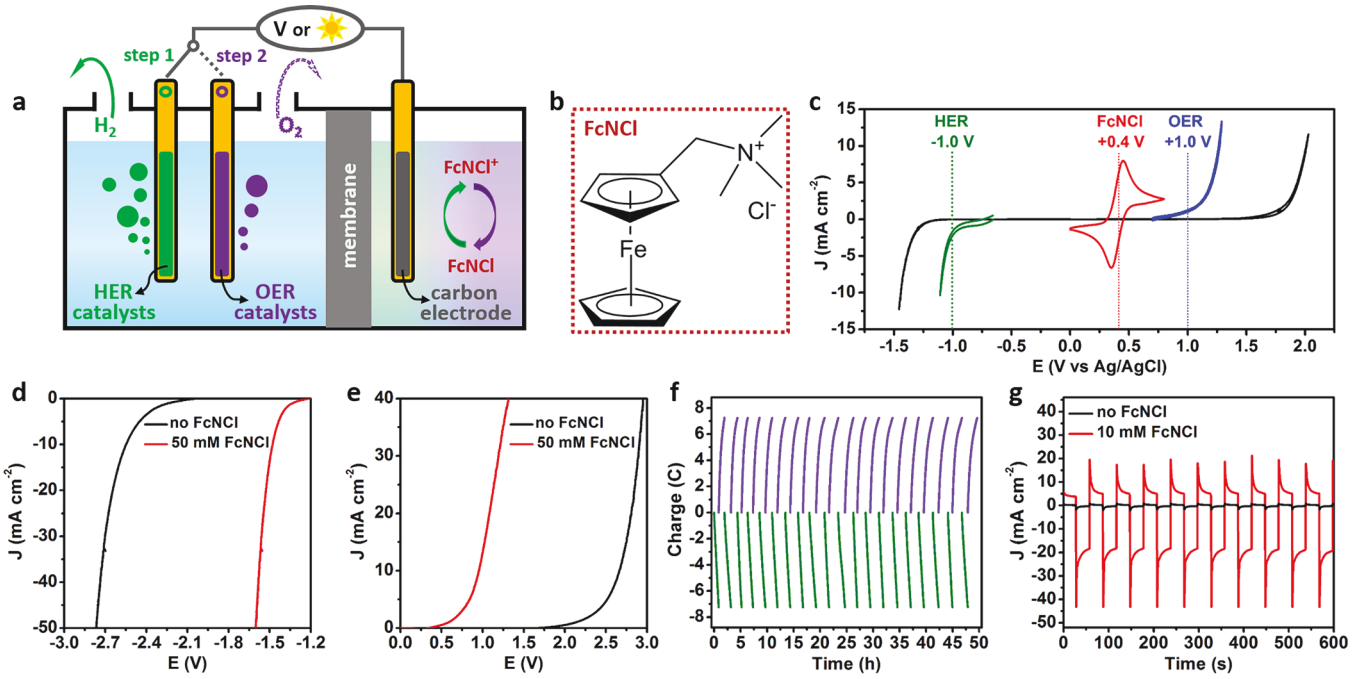

Figure 5. (a) Scheme of FcNCl-mediated decoupled water electrolysis. (b) Chemical structure of FcNCl. (c) Cyclic voltammograms of 50 mM FcNCl (red), HER on glassy carbon (black) and Ni_2P/Ni/NF (green), and OER on glassy carbon (black) and Ni foam (blue) in 0.5 M Na_2SO_4. LSV curves of (d) HER on Ni_2P/Ni/NF and (e) OER on Ni foam in a two-electrode configuration in 0.5 M Na_2SO_4 with and without 50 mM FcNCl in the counter chamber. (f) Charge evolution for repeated decoupled water electrolysis in 0.5 M Na_2SO_4 with 10 mM FcNCl in the counter compartment. Voltage bias between the working and counter electrodes was alternated at −1.6 V for HER and 1.8 V for OER. (g) HER current density on Ni_2P/Ni/NF with and without 10 mM FcNCl in the counter chamber driven by a solar cell under chopped sunlight irradiation. Reproduced from ref 16. Copyright 2018 Elsevier.

least four advantages: (1) Owing to the more favorable thermodynamics of selected organic oxidation reactions, such a hybrid electrolyzer can deliver higher current density with lower voltage input, hence increasing the energy conversion efficiency. (2) The anode side will yield value-added organic products, maximizing the return of energy investment. (3) Since no O_2 will be produced, no H_2/O_2 mixing and reactive oxygen species issues exist. (4) The high selectivity of H_2 production on the cathode side in the presence of organic substrates enables single-compartment membrane-free electrolysis, substantially reducing the cost of electrolyzers. In order to achieve these advantages, an ideal organic substrate should satisfy the following requirements: high solubility in water at room temperature, production of value-added nongaseous product(s) through oxidation, less positive oxidation potential at the anode relative to the onset of OER, and negligible competition with HER at the cathode. Among many biomass-derived intermediates, 5-hydroxymethylfurfural (HMF) stands out as a promising candidate because it can be transformed to various valuable products, including 2,5-furandicarboxylic acid (FDCA) via oxidation (Figure 6a).[20−25] In fact, FDCA has been advocated as a replacement of terephthalic acid for the production of polyamides, polyesters, and polyurethanes.[25]

To our delight, a reported nonprecious bifunctional electrocatalyst for overall water splitting is able to readily catalyze the oxidation of HMF to FDCA in 1.0 M KOH.[21] SEM and elemental mapping images in Figure 6b present the morphology and elemental distribution of the model electrocatalyst, 3D Ni_2P nanoparticle arrays coated on nickel foam (Ni_2P NPA/NF). Linear sweep voltammetry study clearly demonstrates that in the presence of 10 mM HMF, the anodic current takes off at a potential substantially less positive than that of OER (Figure 6c), saving nearly 200 mV voltage input to reach the same current density of 100 mA cm^{-2}. The HMF conversion and product evolution over time are plotted in Figure 6d, confirming the nearly 100% yield of FDCA and its unity Faradaic efficiency. The goal of simultaneously producing H_2 and FDCA necessitates great electrocatalytic activity and selectivity of Ni_2P NPA/NF toward H_2 production even in the presence of HMF. Indeed, as demonstrated in Figure 6e, the cathodic LSV curves of Ni_2P NPA/NF display negligible difference with regard to the addition of 10 mM HMF. The robust stability and preference of Ni_2P NPA/NF for HER versus HMF reduction is further corroborated by a 12 h chronopotentiometry experiment conducted at −10 mA cm^{-2} with 10 mM HMF, showing 100% Faradaic efficiency of H_2 production.[21] The foregoing results were obtained in a three-electrode configuration. When a two-electrode electrolyzer employs Ni_2P NPA/NF as the electrocatalysts for both cathode and anode, simultaneous production of FDCA and H_2 can be realized. As compared in Figure 6f, the LSV curve of HMF oxidation integrated with HER takes off at much smaller voltage input than that of pure water splitting. Nearly 200 mV voltage can be universally saved to reach benchmark current densities of 10, 20, and 50 mA cm^{-2} (Figure 6g). Long-term controlled potential electrolysis conducted at 1.5 V produces H_2 with a yield close to the theoretical predicted amount (Figure 6h), indicative of a unity Faradaic efficiency for HER. In fact, continuously running three repetitive electrolysis cycles using the same Ni_2P NPA/NF catalyst couple shows no degradation of the electrocatalysts, and they retain great activity, selectivity, and robustness for both HER and HMF oxidation to FDCA (Figure 6i).

DOI: 10.1021/acs.accounts.8b00002
Acc. Chem. Res. 2018, 51, 1571−1580

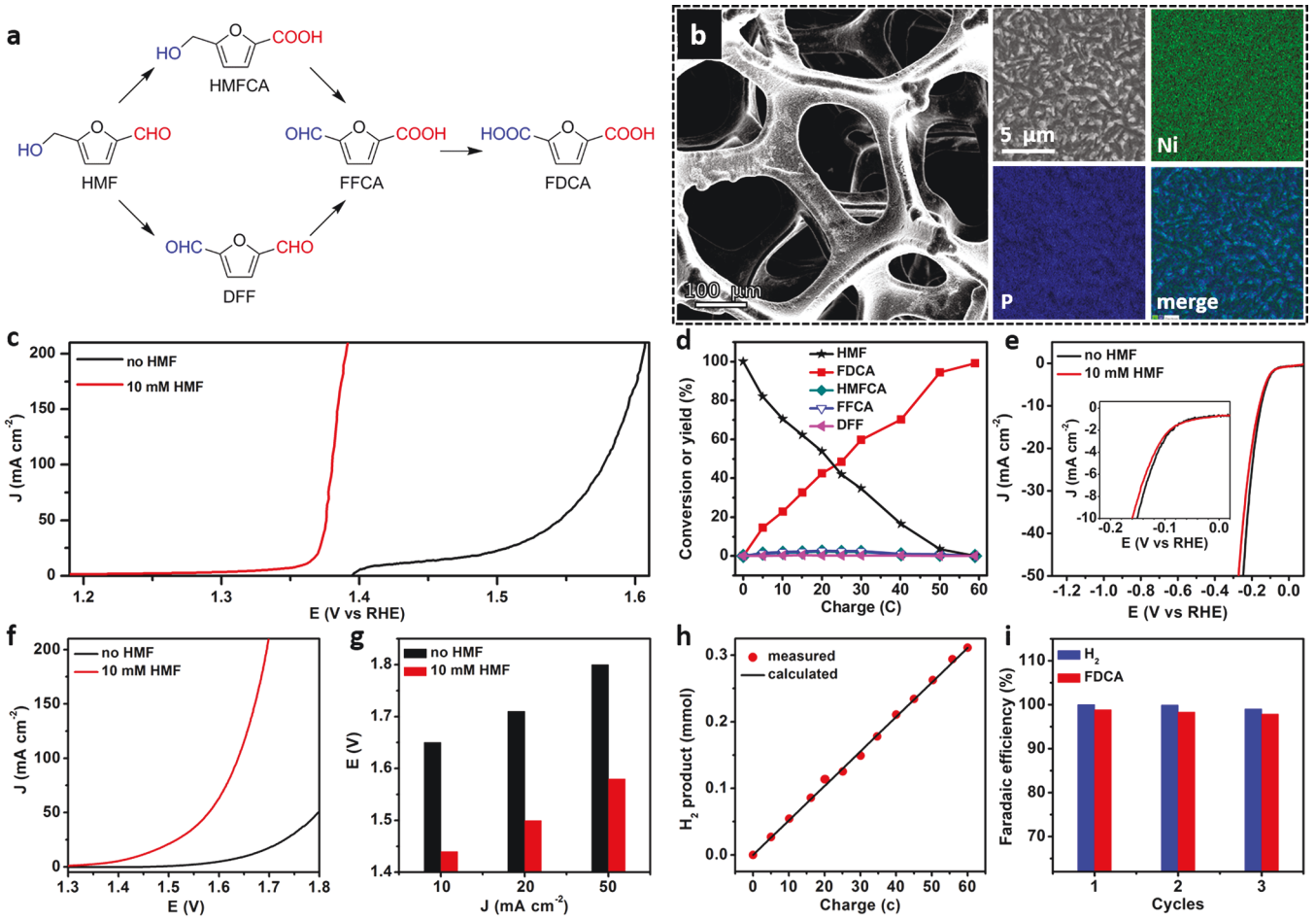

Figure 6. (a) Two possible pathways of HMF oxidation to FDCA. (b) SEM and elemental mapping images of Ni_2P NPA/NF. (c) LSV curves of Ni_2P NPA/NF in 1.0 M KOH with and without 10 mM HMF. (d) HMF conversion and product evolution during electrolysis at 1.423 V vs RHE in 1.0 M KOH with 10 mM HMF. (e) LSV curves of Ni_2P NPA/NF in 1.0 M KOH with and without 10 mM HMF. (f) LSV curves and (g) comparison of the cell voltages to achieve benchmark current densities using a Ni_2P NPA/NF catalyst couple in 1.0 M KOH with and without 10 mM HMF. (h) GC-measured H_2 quantity compared with that theoretically calculated assuming a 100% Faradaic efficiency. (i) Faradaic efficiencies of the Ni_2P NPA/NF catalyst couple for simultaneous H_2 and FDCA generation in 1.0 M KOH with 10 mM HMF for three successive electrolysis cycles. Reproduced from ref 21. Copyright 2016 John Wiley & Sons, Inc.

Encouraged by the above results and thanks to the modular nature of hybrid water electrolysis, we were able to explore the electrocatalytic upgrading of a diverse array of biomass-derived intermediate compounds (e.g., ethanol, benzyl alcohol, furfural, and furfuryl alcohol) and the utilization of nonprecious bifunctional electrocatalysts (e.g., transition metals, sulfides, phosphides, etc.).[23,24] In fact, the large anodic potential requirement of OER leaves us a wide potential window to carry out desirable organic oxidation reactions without the formation of O_2 in aqueous media. For instance, Figure 7a–e presents five representative organic oxidation reactions together with their corresponding LSV curves on 3D Ni_3S_2/NF (Figure 7f). All of these reactions take place at potentials less positive than that of OER, consistent with their more favorable thermodynamics under alkaline conditions. One interesting observation is that their catalytic currents take off at very similar potentials (~1.36 V vs RHE), regardless of the intrinsic thermodynamic difference of each organic reaction. In order to avoid the potential influence of nonmetal elements in the catalyst composition, we purposely fabricated a highly porous Ni foam (hp-Ni) as the working electrode (Figure 7g). Subsequently, benzyl alcohol with different electronic substituents was selected as the organic substrate (Figure 7h). One would expect an electron-donating moiety such as a methyl group should enable the oxidation to occur at a more negative potential while an electron-withdrawing group like a $-NO_2$ group should shift the oxidation potential more positively. However, regardless of the different substituents at the para-position of the phenyl ring in benzyl alcohol, these three substrates exhibit almost identical LSV curves for oxidation on hp-Ni (Figure 7i). These preliminary results prompt us to hypothesize that these alcohol oxidation reactions on solid-state electrocatalysts like hp-Ni is primarily determined by the potential to achieve the desirable oxidation state of the catalyst, rather than the intrinsic thermodynamics of each organic oxidation, in contrast to typical homogeneous oxidation reactions catalyzed by molecular catalysts.

2.4. Tandem Water Electrolysis

One challenge of the wide deployment of H_2 utilization is its cost-effective storage and transport.[36,37] A potential strategy to bypass this challenge is directly consuming H_2 during water electrolysis to produce value-added chemical fuels (e.g., CH_4, NH_3, etc.) via biological catalysts (i.e., enzymes); within this context tandem water electrolysis emerges (Figure 2d).

DOI: 10.1021/acs.accounts.8b00002
Acc. Chem. Res. 2018, 51, 1571−1580

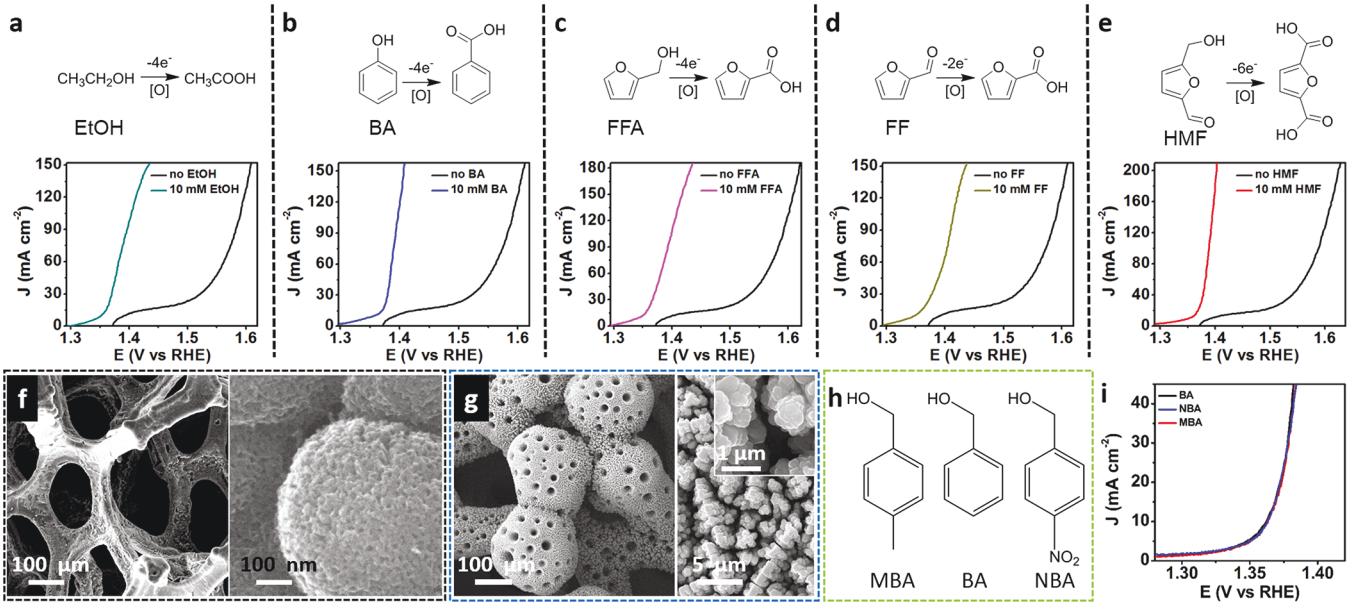

Figure 7. (a–e) Oxidation of selected organics to value-added products and their corresponding LSV curves on Ni_3S_2/NF in 1.0 M KOH (BA, benzyl alcohol; FFA, furfuryl alcohol; FF, furfural; HMF, 5-hydroxymethylfurfural). SEM images of (f) Ni_3S_2/NF and (g) hp-Ni. (h) Chemical structures of MBA, BA, and NBA. (i) LSV curves on hp-Ni in 1.0 M KOH with 10 mM MBA, BA, and NBA. Panels a–f reproduced from ref 23. Copyright 2016 American Chemical Society. Panels g–i reproduced from ref 24. Copyright 2017 American Chemical Society.

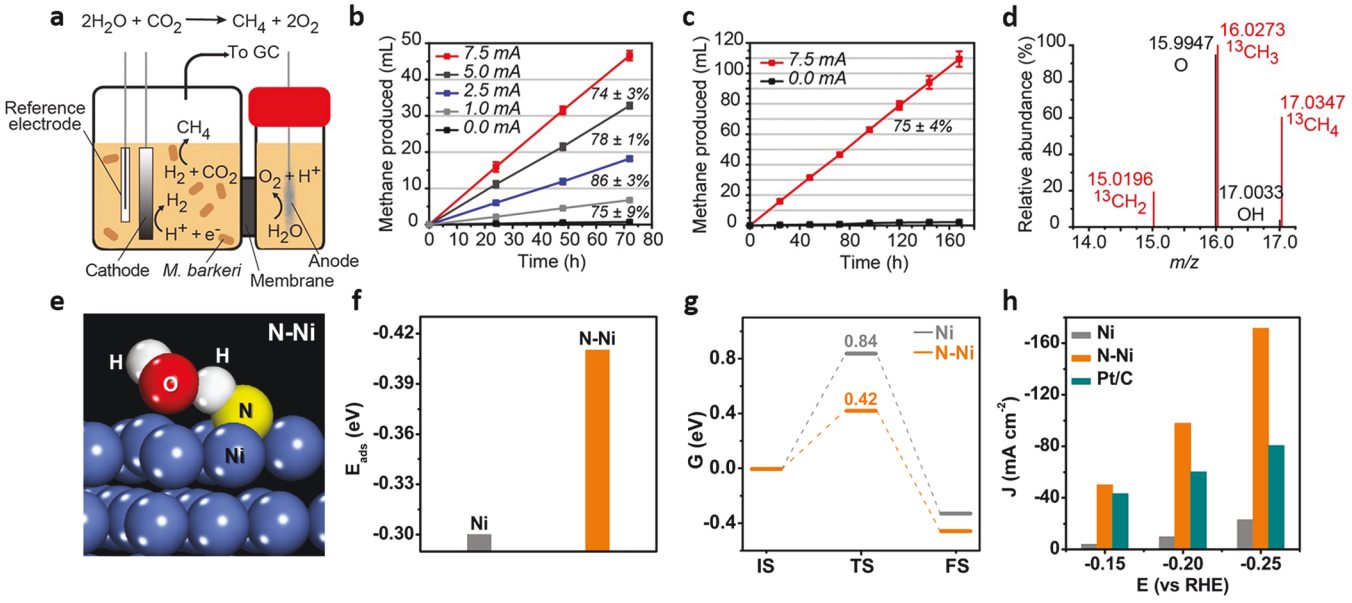

Figure 8. (a) Scheme of tandem water electrolysis. (b, c) CH_4 production and Faradaic efficiency with varying applied current. (d) High-resolution mass spectrometry analysis of gas products. (e) Optimized structure of water adsorption on N–Ni(111). (f) Adsorption energy of water on Ni(111) and N–Ni(111). (g) Free energy barrier profiles of water dissociation on Ni(111) and N–Ni(111). (h) Comparison of the current densities at different overpotentials for N–Ni, Ni framework, and Pt/C for HER under neutral conditions. Panels a–d reproduced from ref 36. Copyright 2015 National Academy of Sciences of the United States of America. Panels e–h reproduced from ref 39. Copyright 2017 American Chemical Society.

Figure 8a schematically depicts the concept of tandem water electrolysis, wherein an airtight two-compartment electrochemical cell is charged with *Methanosarcina barkeri* (*M. barkeri*) and CO_2 in the cathodic chamber.[36] Sustainable electricity or solar input or both drives water splitting using inorganic catalysts to produce H_2, which is consumed by *M. barkeri* in the presence of CO_2 to produce CH_4. After galvanostatic electrolysis for 11.5 h and sampling for 0.5 h, the GC analysis of gas products revealed that CH_4 production linearly and cumulatively increased under all the applied currents (1.0–7.5 mA) with an average Faradaic efficiency above 74% (Figure 8b). The proportion of CH_4 production to the applied current suggests that electrocatalytic H_2 production is the rate-limiting step of the entire system. As *M. barkeri* operates at a nearly thermodynamic potential, the only overpotential involved is due to HER in neutral aqueous medium (1.0 M phosphate buffer). Such a hybrid bioinorganic system for tandem water electrolysis shows robust durability, producing CH_4 at a constant rate over 7 days with a Faradaic efficiency close to 75% (Figure 8c). The carbon source for CH_4

DOI: 10.1021/acs.accounts.8b00002
Acc. Chem. Res. 2018, 51, 1571–1580

is indeed the original CO_2 as confirmed by an isotope labeling experiment. When $^{13}CO_2$ was utilized during electrocatalysis, only $^{13}CH_4$ was detected via high-resolution mass spectrometry (Figure 8d), whereas only $^{12}CH_4$ was observed if $^{12}CO_2$ used instead. In terms of electrocatalysts for the in situ H_2 production, this hybrid system possesses high flexibility. A variety of earth-abundant and biocompatible inorganic electrocatalysts can be utilized, such as NiS and NiMo. Once integrated with photoelectrodes, direct solar-to-chemical conversion is also feasible based upon this tandem water electrolysis strategy.[36]

Recently, Nocera et al. reported a similar hybrid water splitting−biosynthetic system utilizing Co−P as the inorganic HER catalyst and *Ralstonia eutropha* as the biocatalyst.[37] The overall energy conversion efficiency was reported to be higher than that of photosynthesis. An alternative tandem water electrolysis system was also reported by the same group, wherein H_2-oxidizing autotrophic bacterium *Xanthobacter autotrophicus* was employed and NH_3 was produced from N_2 and H_2O.[38]

In order to be fully compatible with biological systems for tandem water electrolysis, an ideal reaction medium is neutral water. However, most earth-abundant HER electrocatalysts exhibit mediocre performance under neutral conditions.[11,29,30,39] Our group recently reported a general surface nitrogen modification strategy to considerably enhance the activity of first-row transition metals (e.g., Fe, Co, Ni, Cu, and NiCo alloy) for electrocatalytic H_2 evolution in neutral aqueous buffer.[39] In particular, the resulting N−Ni electrocatalyst rivals commercially available Pt/C for HER at pH 7. Detailed physical characterizations reveal that the bulk composite of N−Ni retains metallic nickel, whereas nitrogen only exists on the catalyst surface in the formation of "surface nitrides". Density functional theory computation suggests that the surface nitrogen is likely positioned at the hollow fcc site of nickel and bound to three surface nickel atoms (Figure 8e). It is widely acknowledged that water adsorption and dissociation are critical steps for HER under neutral and alkaline conditions. An ideal HER electrocatalyst should have sufficient affinity to bind water to accelerate the initial electron-transfer process but also possess enough repellency to facilitate the subsequent water dissociation. Figure 8f compares the adsorption energy (E_{ads}) of water on Ni (−0.30 eV) vs N−Ni (−0.41 eV). It is apparent that the presence of N in N−Ni facilitates water adsorption wherein the hydrogen bond is naturally invoked. Furthermore, the free energy barrier for water dissociation on N−Ni is predicted theoretically at 0.42 eV (Figure 8g), also substantially lower than that on pure nickel (0.84 eV). Taken together, the surface nitrogen modification has been experimentally and theoretically proven as an effective approach to boost HER under neutral conditions. As highlighted in Figure 8h, N−Ni even exhibits superior HER activity at pH 7 to that of Pt/C, not even to mention pure nickel and other nonprecious electrocatalysts reported so far, rendering N−Ni an excellent HER electrocatalyst to integrate with many biological systems for tandem water electrolysis and beyond.

3. SUMMARY AND OUTLOOK

This Account has summarized recent advances in four innovative strategies for nonconventional water splitting, circumventing many challenges in traditional water electrolysis and showcasing various advantages. In this burgeoning field, many opportunities await further investigation. For instance, most nonprecious bifunctional electrocatalysts for overall water splitting only function well in alkaline (and neutral) electrolytes. Nearly no low-cost electrocatalyst couples have been reported for water electrolysis at low pH. Along with the success in proton-exchange membrane and high conductivity of acidic electrolytes, it is very appealing to conduct water electrolysis under low pH conditions with earth-abundant electrocatalysts. In addition, most nonprecious electrocatalysts will undergo surface (if not bulk) oxidation during OER; hence the real active sites are usually different from those on the original catalysts. How to rationally control and understand such in situ oxidation to yield active sites while still retaining highly conductive bulk composite necessitates further research. The synthetic cost of redox mediators should also be further reduced to be economically attractive for large-scale decoupled water electrolysis. In particular, solubility, stability, and fast electron transfer kinetics of redox mediators are critical factors determining their potential for practical applications. For hybrid water electrolysis, high selectivity for desirable products from those selected organic oxidations should be the primary goal, and the subsequent separation and purification should also be taken into account. As organic electrocatalysis and electrosynthesis is about to witness a renaissance, we are optimistic that integrating many promising organic oxidation reactions (e.g., oxidative C−C coupling) will burgeon in this field.[40] It is exciting to see recent successes in tandem water electrolysis integrating biological enzymes to yield highly valuable products from inert starting molecules like CO_2 and N_2. Nevertheless, the long-term stability, scalability, and overall cost of these bioinorganic electrocatalytic systems should be thoroughly analyzed prior to practical implementation. We hope this Account will encourage more efforts into the development of advanced electrocatalysts and the design of novel strategies for H_2 production and more importantly organic upgrading under benign conditions.

AUTHOR INFORMATION

Corresponding Authors

*E-mail: youbo@mail.ustc.edu.cn.
*E-mail: yujie.sun@usu.edu.

ORCID

Bo You: 0000-0003-1849-0418
Yujie Sun: 0000-0002-4122-6255

Notes

The authors declare no competing financial interest.

Biographies

Bo You received his B.S. degree in Chemistry in 2008 from Heilongjiang University and a Ph.D. degree under the supervision of Prof. Zhaoxiang Deng at University of Science and Technology of China (USTC) in 2014. After the postdoctoral positions in Prof. Yujie Sun's group at Utah State University and Prof. Hong Li's group at Nanyang Technological University, he joined Prof. Shi-Zhang Qiao's group as an ARC Research Associate at The University of Adelaide. His research interests include inorganic catalysts for advanced renewable energy (ICARE).

Yujie Sun obtained his B.S. degree in Chemistry from Fudan University in 2005. He then pursued graduate studies with Prof. Claudia Turro at The Ohio State University and was awarded a Ph.D. degree in 2010. Subsequently, he conducted a postdoctoral stint with Prof. Christopher J. Chang at the University of California, Berkeley,

DOI: 10.1021/acs.accounts.8b00002
Acc. Chem. Res. 2018, 51, 1571−1580

and Lawrence Berkeley National Laboratory. He started his independent academic career at Utah State University in 2013. His group is interested in developing and understanding inexpensive materials and complexes with applications related to energy and health.

■ ACKNOWLEDGMENTS

Y.S. acknowledges the financial support of Utah State University, USTAR of the State of Utah, Ralph E. Powe Junior Faculty Enhancement Award from Oak Ridge Associated Universities, Inc., and National Science Foundation (CAREER Award, CHE-1653978).

■ REFERENCES

(1) Lewis, N. S.; Nocera, D. G. Powering the Planet: Chemical Challenges in Solar Energy Utilization. *Proc. Natl. Acad. Sci. U. S. A.* **2006**, *103*, 15729−15735.
(2) Hunter, B. M.; Gray, H. B.; Müller, A. M. Earth-Abundant Heterogeneous Water Oxidation Catalysts. *Chem. Rev.* **2016**, *116*, 14120−14136.
(3) Chu, S.; Majumdar, A. Opportunities and Challenges for A Sustainable Energy Future. *Nature* **2012**, *488*, 294−303.
(4) Jiao, Y.; Zheng, Y.; Jaroniec, M.; Qiao, S. Z. Design of Electrocatalysts for Oxygen- and Hydrogen-Involving Energy Conversion Reactions. *Chem. Soc. Rev.* **2015**, *44*, 2060−2086.
(5) You, B.; Sun, Y. Chalcogenide and Phosphide Solid-State Catalysts for H_2 Generation. *ChemPlusChem* **2016**, *81*, 1045−1055.
(6) Zhu, Y. P.; Guo, C.; Zheng, Y.; Qiao, S. Z. Surface and Interface Engineering of Noble-Metal-Free Electrocatalysts for Efficient Energy Conversion Processes. *Acc. Chem. Res.* **2017**, *50*, 915−923.
(7) Carmo, M.; Fritz, D. L.; Mergel, J.; Stolten, D. A Comprehensive Review on PEM Water Electrolysis. *Int. J. Hydrogen Energy* **2013**, *38*, 4901−4934.
(8) Jiang, N.; You, B.; Sheng, M.; Sun, Y. Electrodeposited Cobalt-Phosphorous-Derived Films as Competent Bifunctional Catalysts for Overall Water Splitting. *Angew. Chem., Int. Ed.* **2015**, *54*, 6251−6254.
(9) Jiang, N.; You, B.; Sheng, M.; Sun, Y. Bifunctionality and Mechanism of Electrodeposited Nickel-Phosphorous Films for Efficient Overall Water Splitting. *ChemCatChem* **2016**, *8*, 106−112.
(10) You, B.; Jiang, N.; Sheng, M.; Bhushan, M. W.; Sun, Y. Hierarchically Porous Urchin-Like Ni_2P Superstructures Supported on Nickel Foam as Efficient Bifunctional Electrocatalysts for Overall Water Splitting. *ACS Catal.* **2016**, *6*, 714−721.
(11) You, B.; Sun, Y. Hierarchically Porous Nickel Sulfide Multifunctional superstructures. *Adv. Energy Mater.* **2016**, *6*, 1502333.
(12) You, B.; Jiang, N.; Sheng, M.; Gul, S.; Yano, J.; Sun, Y. High-Performance Overall Water Splitting Electrocatalysts Derived from Cobalt-Based Metal-Organic Frameworks. *Chem. Mater.* **2015**, *27*, 7636−7642.
(13) Liu, X.; You, B.; Sun, Y. Facile Surface Modification of Ubiquitous Stainless Steel Led to Competent Electrocatalysts for Overall Water Splitting. *ACS Sustainable Chem. Eng.* **2017**, *5*, 4778−4784.
(14) Rausch, B.; Symes, M. D.; Chisholm, G.; Cronin, L. Decoupled Catalytic Hydrogen Evolution from A Molecular Metal Oxide Redox Mediator in Water Splitting. *Science* **2014**, *345*, 1326−1330.
(15) Symes, M. D.; Cronin, L. Decoupling Hydrogen and Oxygen Evolution during Electrolytic Water Splitting Using An Electron-Coupled-Proton Buffer. *Nat. Chem.* **2013**, *5*, 403−409.
(16) Li, W.; Jiang, N.; Hu, B.; Liu, X.; Song, F.; Han, G.; Jordan, T. J.; Hanson, T. B.; Liu, T. L.; Sun, Y. Electrolyzer Design for Flexible Decoupled Water Splitting and Organic Upgrading with Electron Reservoirs. *Chem.* **2018**, *4*, 637−649, DOI: 10.1016/j.chempr.2017.12.019.
(17) Rausch, B.; Symes, M. D.; Cronin, L. A Bio-Inspired, Small Molecule Electron-Coupled-Proton Buffer for Decoupling the Half-Reactions of Electrolytic Water Splitting. *J. Am. Chem. Soc.* **2013**, *135*, 13656−13659.
(18) Chen, L.; Dong, X.; Wang, Y.; Xia, Y. Separating Hydrogen and Oxygen Evolution in Alkaline Water Electrolysis Using Nickel Hydroxide. *Nat. Commun.* **2016**, *7*, 11741.
(19) Landman, A.; Dotan, H.; Shter, G. E.; Wullenkord, M.; Houaijia, A.; Maljusch, A.; Grader, G. S.; Rothschild, A. Photoelectrochemical Water Splitting in Separate Oxygen and Hydrogen Cells. *Nat. Mater.* **2017**, *16*, 646−651.
(20) Han, G.; Jin, Y. H.; Burgess, R. A.; Dickenson, N. E.; Cao, X. M.; Sun, Y. Visible-Light-Driven Valorization of Biomass Intermediates Integrated with H_2 Production Catalyzed by Ultrathin Ni/CdS Nanosheets. *J. Am. Chem. Soc.* **2017**, *139*, 15584−15587.
(21) You, B.; Jiang, N.; Liu, X.; Sun, Y. Simultaneous H_2 Generation and Biomass Upgrading in Water by An Efficient Noble-Metal-Free Bifunctional Electrocatalyst. *Angew. Chem., Int. Ed.* **2016**, *55*, 9913−9917.
(22) Jiang, N.; You, B.; Boonstra, R.; Terrero Rodriguez, I. M.; Sun, Y. Integrating Electrocatalytic 5-Hydroxymethylfurfural Oxidation and Hydrogen Production via Co-P-Derived Electrocatalysts. *ACS Energy Lett.* **2016**, *1*, 386−390.
(23) You, B.; Liu, X.; Jiang, N.; Sun, Y. A General Strategy for Decoupled Hydrogen Production from Water Splitting by Integrating Oxidative Biomass Valorization. *J. Am. Chem. Soc.* **2016**, *138*, 13639−13646.
(24) You, B.; Liu, X.; Liu, X.; Sun, Y. Efficient H_2 Evolution Coupled with Oxidative Refining of Alcohols via A Hierarchically Porous Nickel Bifunctional Electrocatalyst. *ACS Catal.* **2017**, *7*, 4564−4570.
(25) Cha, H. G.; Choi, K. S. Combined Biomass Valorization and Hydrogen Production in A Photoelectrochemical Cell. *Nat. Chem.* **2015**, *7*, 328−333.
(26) Murray, L. J.; Dincă, M.; Long, R. R. Hydrogen Storage in Metal-Organic Frameworks. *Chem. Soc. Rev.* **2009**, *38*, 1294−1314.
(27) Struzhkin, V. V.; Militzer, B.; Mao, W. L.; Mao, H.; Hemley, R. J. Hydrogen Storage in Molecular Clathrates. *Chem. Rev.* **2007**, *107*, 4133−4151.
(28) Luo, J.; Vermaas, D. A.; Bi, D.; Hagfeldt, A.; Smith, W. A.; Grätzel, M. Bipolar Membrane-Assisted Solar Water Splitting in Optimal pH. *Adv. Energy Mater.* **2016**, *6*, 1600100.
(29) Sun, Y.; Liu, C.; Grauer, D. C.; Yano, J.; Long, J. R.; Yang, P.; Chang, C. J. Electrodeposited Cobalt-Sulfide Catalyst for Electrochemical and Photoelectrochemical Hydrogen Generation from Water. *J. Am. Chem. Soc.* **2013**, *135*, 17699−17702.
(30) Jiang, N.; Bogoev, L.; Popova, M.; Gul, S.; Yano, J.; Sun, Y. Electrodeposited Nickel-Sulfide Films as Competent Hydrogen Evolution Catalysts in Neutral Water. *J. Mater. Chem. A* **2014**, *2*, 19407−19414.
(31) Li, W.; Liu, J.; Zhao, D. Mesoporous Materials for Energy Conversion and Storage Devices. *Nat. Rev. Mater.* **2016**, *1*, 16023.
(32) You, B.; Jiang, N.; Sheng, M.; Sun, Y. Microwave vs. Solvothermal Synthesis of Hollow Cobalt Sulfide Nanoprisms for Electrocatalytic Hydrogen Evolution and Supercapacitors. *Chem. Commun.* **2015**, *51*, 4252−4255.
(33) You, B.; Jiang, N.; Sheng, M.; Drisdell, W. S.; Yano, J.; Sun, Y. Bimetal-Organic Framework Self-Adjusted Synthesis of Support-Free Nonprecious Electrocatalysts for Efficient Oxygen Reduction. *ACS Catal.* **2015**, *5*, 7068−7076.
(34) Lee, K. J.; Lee, J. H.; Jeoung, S.; Moon, H. R. Transformation of Metal-Organic Frameworks/Coordination Polymers into Functional Nanostructured Materials: Experimental Approaches Based on Mechanistic Insights. *Acc. Chem. Res.* **2017**, *50*, 2684−2692.
(35) Jamesh, M. I. Recent Progress on Earth Abundant Hydrogen Evolution Reaction and Oxygen Evolution Reaction Bifunctional Electrocatalyst for Overall Water Splitting in Alkaline Media. *J. Power Sources* **2016**, *333*, 213−236.
(36) Nichols, E. M.; Gallagher, J. J.; Liu, C.; Su, Y.; Resasco, J.; Yu, Y.; Sun, Y.; Yang, P.; Chang, M. C. Y.; Chang, C. J. Hybrid Bioinorganic Approach to Solar-to-Chemical Conversion. *Proc. Natl. Acad. Sci. U. S. A.* **2015**, *112*, 11461−11466.

DOI: 10.1021/acs.accounts.8b00002
Acc. Chem. Res. 2018, 51, 1571−1580

(37) Liu, C.; Colón, B. C.; Ziesack, M.; Silver, P. A.; Nocera, D. G. Water Splitting-Biosynthetic System with CO2 Reduction Efficiencies Exceeding Photosynthesis. *Science* **2016**, *352*, 1210−1213.
(38) Liu, C.; Sakimoto, K. K.; Colón, B. C.; Silver, P. A.; Nocera, D. G. Ambient Nitrogen Reduction Cycle Using A Hybrid Inorganic-Biological System. *Proc. Natl. Acad. Sci. U. S. A.* **2017**, *114*, 6450−6455.
(39) You, B.; Liu, X.; Hu, G.; Gul, S.; Yano, J.; Jiang, D. E.; Sun, Y. Universal Surface Engineering of Transition Metals for Superior Electrocatalytic Hydrogen Evolution in Neutral Water. *J. Am. Chem. Soc.* **2017**, *139*, 12283−12290.
(40) Shi, W.; Liu, C.; Lei, A. Transition-Metal Catalyzed Oxidative Cross-Coupling Reaction to Form C-C Bonds Involving Organometallic Reagents as Nucleophiles. *Chem. Soc. Rev.* **2011**, *40*, 2761−2776.

DOI: 10.1021/acs.accounts.8b00002
Acc. Chem. Res. 2018, 51, 1571−1580